

Input-to-State Stable Integral Line-of-Sight Guidance for Curved Paths with Anti-Windup Guarantees

Henrik M. Schmidt-Didlaukies[‡], Erlend A. Basso[‡], and Kristin Y. Pettersen

Abstract—This letter considers integral line-of-sight (LOS) guidance for curved path following for underactuated marine vehicles. The proposed guidance scheme renders the resulting closed-loop system input-to-state stable (ISS) with respect to a function of the vehicle’s velocities. Moreover, if the forward and sideways velocities are proportional, we show that the origin of the closed-loop system is uniformly globally asymptotically stable (UGAS). Remarkably, these results are derived without the standard assumption of a small crab angle. Furthermore, we discuss how the path parameter should be selected to ensure that the along-track error remains zero for all time, and we show the connection between selecting the path parameter through differential equations and optimization. Finally, we demonstrate the effectiveness of the proposed approach through numerical simulations of an underwater vehicle.

I. INTRODUCTION

Line-of-sight (LOS) guidance laws are ubiquitous in the literature on path following for underactuated marine vehicles. There are two main types of LOS guidance laws: static feedback proportional LOS guidance laws and dynamic feedback integral LOS (ILOS) guidance laws. As the names suggest, the latter includes an integral state while the former is a purely static state feedback control law. There is an extensive amount of literature on the subject of LOS guidance for marine vehicles, and the reader is referred to the recent survey [1] and the references therein. The following review is limited to LOS guidance algorithms with integral action.

The classical ILOS guidance law for marine vehicles is introduced in [2]. This work proves global asymptotic path following under the assumption that the path is a straight line and that the integral gain is sufficiently small relative to the forward velocity. The guidance law is tested experimentally with an uncrewed semi-submersible vehicle and an autonomous underwater vehicle (AUV) in [3], [4]. Another application of the classical ILOS guidance law is found in [5], where it is used in the control system of an underwater snake robot.

The adaptive ILOS (AILOS) guidance law is presented in [6]. The AILOS guidance law differs from the classical ILOS guidance law in that the integral state update is structurally different. The work shows global asymptotic path following under the assumption that the vehicle crab angle is small

and constant. The restriction placed on the integral gain is independent of the vehicle velocity, which suggests that the guidance law is applicable to vehicles operating in different speed regimes. An equivalent guidance law is given in [7], but global asymptotic path following is not proven for nonzero crab angles.

An extended-state-observer-based LOS (ELOS) guidance law is proposed in [8]. Under the assumption of a small crab angle, the authors provide an input-to-state stability (ISS) [9] result for the closed-loop system with respect to the crab angle estimation error. However, since the crab angle estimation error is not shown to converge, global asymptotic path following for a constant crab angle is not proven. More recently, the work [10] introduced the adaptive LOS (ALOS) guidance law. Unlike previous approaches, the integral state represents an estimate of the crab angle directly. However, since the integral state is not bounded, the resulting control law can exhibit unwinding. The latter problem is addressed in [11], where a projection operator is employed to ensure that the integral state is bounded. Semi-global tracking of the guidance law is proven. However, no relationship between the region of attraction and the control gains or system parameters is given.

When analyzed in a kinematic setting, all of the aforementioned LOS guidance approaches ensuring global asymptotic path following have one major assumption in common, which is the small crab angle assumption. While this may be a reasonable assumption for ships for which the speed of the vehicle is significantly larger than the ocean current speed, it is not necessarily true for smaller uncrewed vehicles such as torpedo-shaped underwater vehicles. Moreover, the small crab angle assumption is easily violated if the reference paths are curved.

The main contributions of this letter are twofold: 1) We discuss how the path parameter should be selected to ensure that the along-track error remains zero at all times. In particular, we show the relationship between selecting the path parameter through an ordinary differential equation (ODE) and through an optimization problem, and we discuss the practical effects this can have for implementation purposes. 2) We introduce a novel ILOS-type guidance law. A key advantage of the proposed guidance law compared to most other approaches in the literature is that the integral state is bounded. Additionally, we provide an ISS result for the closed-loop system with respect to a function of the vehicle velocities. As a result, if the forward and sideways velocities are proportional, we show that the origin of the closed-loop system is uniformly globally asymptotically stable (UGAS). A key novelty in the proof is that we show UGAS without

This work was supported by the European Research Council (ERC) under the European Union’s Horizon 2020 research and innovation programme, through the ERC Advanced Grant 101017697-CRÈME, and by the Research Council of Norway through the Centres of Excellence funding scheme, project No. 223254, NTNU AMOS.

[‡] H. M. Schmidt-Didlaukies and E. A. Basso contributed equally to this work and should be considered co-first authors

The authors are with the Department of Engineering Cybernetics, Norwegian University of Science and Technology, NO-7491 Trondheim, Norway {henrik.schmidt,erlend.a.basso,kristin.y.pettersen}@ntnu.no

assuming that the crab angle is small. Moreover, we also provide novel upper bounds on the cross-track error, which can be employed to estimate an upper bound on the allowed curvature of the path. Together, these bounds can ensure that all maximal solutions to the path selection ODE are complete.

This letter is organized as follows. Section II introduces the kinematic model of a vehicle operating in the plane, several concepts related to paths, and the problem statement. In Section III, we demonstrate how the path parameter can be selected to ensure that the along-track error remains zero for all time. Moreover, we discuss the connection between selecting the path parameter through an ODE and through an optimization problem. Section IV presents the novel projection-based ILOS guidance algorithm and the associated stability proofs. Finally, Section V presents a case study that demonstrates the effectiveness of the results in simulation for an autonomous underwater vehicle.

Notation: The Euclidean inner product in \mathbb{R}^n is written $\langle x, y \rangle$, and the Euclidean norm is denoted $|x| = \langle x, x \rangle^{1/2}$. The unit circle is defined by $\mathbb{S} := \{x \in \mathbb{R}^2 : |x| = 1\}$, and the group of planar rotations by $\text{SO}(2) := \{R \in \mathbb{R}^{2 \times 2} : R^T R = I, \det R = 1\}$. A unit vector $z \in \mathbb{S}$ maps to a rotation matrix through the map $R : \mathbb{S} \rightarrow \text{SO}(2)$ defined by $R(z) := (z \ S z)$, where $S := \begin{pmatrix} 0 & -1 \\ 1 & 0 \end{pmatrix}$. Lastly, $\text{atan2} : \mathbb{R}^2 \setminus \{0\} \rightarrow (-\pi, \pi]$ denotes the four-quadrant inverse of tan.

II. MODELING, PATHS, AND PROBLEM STATEMENT

Let $p \in \mathbb{R}^2$ denote the horizontal position of a marine vehicle and let $u = (u_1, u_2) \in \mathbb{R}^2$ denote the forward and sideways velocities, u_1 and u_2 , respectively. The kinematic differential equation is given by

$$\dot{p} = R(z)u = u_1 z + u_2 S z, \quad (p, z, u) \in \mathbb{R}^2 \times \mathbb{S} \times U, \quad (1)$$

where $z \in \mathbb{S}$ represents the orientation of the vehicle and is considered a control input. Moreover, $U := \{u \in \mathbb{R}^2 : u_1 \geq \rho\}$, where $\rho > 0$ is a lower bound on the forward velocity. Observe that if the sideways velocity u_2 is identically equal to zero, then (1) reduces to a unicycle model, which is often used to model a marine vehicle in transit, see e.g. [12], [13]. Hence, the sideways velocity u_2 can also be considered a disturbance, perturbing the model away from the ideal unicycle model.

In this letter, a path is a continuous mapping $\gamma : \mathbb{R} \rightarrow \mathbb{R}^2$. It should be remarked that mathematicians typically refer to such an object as a curve, while the notion of a path is reserved for a curve whose domain is a compact interval. A formal introduction to the geometry of curves is found in [14]. Continuity of γ in itself is not enough to derive the results presented in this letter. The notion of regularity we require is provided by the following definition.

Definition 1. Let $r \geq 1$. A path $\gamma : \mathbb{R} \rightarrow \mathbb{R}^2$ is \mathcal{C}^r regular if

- it is \mathcal{C}^r ;
- it holds that $\gamma'(\theta) \neq 0$ for all $\theta \in \mathbb{R}$;
- the arc length $\ell : \mathbb{R} \rightarrow \mathbb{R}$, defined by

$$\ell(\theta) := \int_0^\theta |\gamma'(\eta)| d\eta, \quad (2)$$

satisfies $\ell(\mathbb{R}) = \mathbb{R}$.

Regularity in the sense of Definition 1 entails that γ is \mathcal{C}^r and that its arc length ℓ is a \mathcal{C}^r diffeomorphism from \mathbb{R} to \mathbb{R} . As a consequence, the arc length reparametrization of γ , that is $\theta \mapsto \gamma(\ell^{-1}(\theta))$, is itself a \mathcal{C}^r regular path. If a path is \mathcal{C}^1 , then ℓ exists and the last condition in Definition 1 is equivalent to

$$\lim_{\theta \rightarrow -\infty} \ell(\theta) = -\infty, \quad \lim_{\theta \rightarrow \infty} \ell(\theta) = \infty. \quad (3)$$

A simple set of sufficient conditions for γ to be \mathcal{C}^r regular is that γ is \mathcal{C}^r and that there exists $\epsilon > 0$ such that $|\gamma'(\theta)| \geq \epsilon$ for all $\theta \in \mathbb{R}$.

If a path is \mathcal{C}^1 regular, then there exists a continuous tangent vector field with unit length, $\tau : \mathbb{R} \rightarrow \mathbb{S}$, defined by

$$\tau(\theta) := \frac{\gamma'(\theta)}{|\gamma'(\theta)|}. \quad (4)$$

Furthermore, if γ is \mathcal{C}^2 regular, then a continuous signed curvature $\kappa : \mathbb{R} \rightarrow \mathbb{R}$ can be defined by

$$\kappa(\theta) := \frac{\langle \tau'(\theta), S\tau(\theta) \rangle}{|\gamma'(\theta)|}. \quad (5)$$

Finally, we note that if γ is parametrized by arc length, that is if $\ell(\theta) = \theta$ or equivalently $|\gamma'(\theta)| = 1$, then the tangent and signed curvature have the simpler expressions $\tau(\theta) = \gamma'(\theta)$ and $\kappa(\theta) = \langle \gamma''(\theta), S\gamma'(\theta) \rangle$, respectively.

The path following problem is to ensure that

$$\lim_{t \rightarrow \infty} |p(t) - \gamma(\theta(t))| = 0. \quad (6)$$

In order to solve the path following problem, we make the coordinate transform

$$\varepsilon(p, \theta) := R(\tau(\theta))^T (p - \gamma(\theta)), \quad (7)$$

where ε represents the position error $p - \gamma(\theta)$ in the path-tangential frame. The components of ε are denoted ε_τ and ε_c and represent the along-track and cross-track errors, respectively. We can rewrite (7) component-wise as

$$\varepsilon_\tau(p, \theta) := \langle p - \gamma(\theta), \tau(\theta) \rangle, \quad (8)$$

$$\varepsilon_c(p, \theta) := \langle p - \gamma(\theta), S\tau(\theta) \rangle. \quad (9)$$

A core idea in LOS guidance is to ensure that the along-track error ε_τ is zero by an appropriate selection of the path parameter θ . Then, (6) reduces to $\lim_{t \rightarrow \infty} |\varepsilon_c(p(t), \theta(t))| = 0$, and the dimension of the workspace \mathbb{R} becomes the same as the dimension of the input space \mathbb{S} .

Problem Statement:

- 1) Select the path parameter $t \mapsto \theta(t)$ such that the along-track error $\varepsilon_\tau(p(t), \theta(t)) = 0$ for all $t \geq 0$.
- 2) Design a control law $z = \mu(p, \theta, \alpha)$, where $\alpha \in \mathbb{R}$ is an integral state, such that the closed-loop system is ISS with respect to a suitable function of u . Moreover, if $u_1 \propto u_2$ then $\varepsilon_c(p(t), \theta(t)) \rightarrow 0$.

III. PATH PARAMETER SELECTION

Consider the set of vehicle positions and path parameters such that the along-track error vanishes,

$$M = \{(p, \theta) \in \mathbb{R}^3 : \varepsilon_\tau(p, \theta) = 0\}. \quad (10)$$

If the path is \mathcal{C}^2 regular, then M is a \mathcal{C}^1 two-dimensional embedded manifold. This is seen by noting that the derivative of ε_τ with respect to (p, θ) does not vanish on M . In particular,

$$\nabla \varepsilon_\tau(p, \theta) = \begin{pmatrix} \tau(\theta) \\ |\gamma'(\theta)|(\kappa(\theta)\varepsilon_c(p, \theta) - 1) \end{pmatrix} \quad (11)$$

for all $(p, \theta) \in \mathbb{R}^3$. The tangent space to M , $\mathbb{T}_M : M \rightarrow \mathbb{R}^3$, is therefore characterized by

$$\mathbb{T}_M(p, \theta) := \{\nu \in \mathbb{R}^3 : \langle \nabla \varepsilon_\tau(p, \theta), \nu \rangle = 0\}. \quad (12)$$

Suppose now that the vehicle travels with velocity $\dot{p} = v$. We select the path parameter by means of a differential relation $\dot{\theta} = \lambda(p, \theta, v)$ such that $(v, \lambda(p, \theta, v)) \in \mathbb{T}_M(p, \theta)$ for all $(p, \theta) \in M$ and all $v \in \mathbb{R}^2$. The resulting system describing the path parameter selection process can be stated as

$$\left. \begin{aligned} \dot{p} &= v \\ \dot{\theta} &= \frac{1}{1 - \kappa(\theta)\varepsilon_c(p, \theta)} \frac{\langle \tau(\theta), v \rangle}{|\gamma'(\theta)|} \end{aligned} \right\} (p, \theta) \in O \cap M, v \in \mathbb{R}^2 \quad (13)$$

where

$$O := \{(p, \theta) \in \mathbb{R}^3 : \kappa(\theta)\varepsilon_c(p, \theta) < 1\}. \quad (14)$$

Remark 1. Similar expressions for λ as given in (13) are also given in works such as [15], [16]. Constraining solutions to lie in the set $O \cap M$ avoids the singularity encountered when the vehicle is situated at a center of curvature, that is, at points $(p, \theta) \in M$ such that $\kappa(\theta)\varepsilon_c(p, \theta) = 1$. The points $(p, \theta) \in M$ such that $\kappa(\theta)\varepsilon_c(p, \theta) > 1$ are also not considered because the vehicle would have to pass through the singularity to reach the path from these points.

While the system (13) describes an exact differential approach to the path parameter selection problem, it is not suitable for practical implementation. In particular, even if θ could be initialized such that $(p, \theta) \in M$, the states would drift out of M due to measurement errors and numerical inaccuracies. However, the following proposition relates the path parameter selection problem to an optimization problem.

Proposition 1. Let γ be a \mathcal{C}^2 regular path. If $(p, \theta_*) \in O \cap M$, then θ_* is a minimum of the function $\theta \mapsto |p - \gamma(\theta)|$.

Proof. Consider the \mathcal{C}^2 function $h_p(\theta) := \frac{1}{2}|p - \gamma(\theta)|^2$, which has the same minima as the function in question. We find that

$$h'_p(\theta) = -\langle p - \gamma(\theta), \gamma'(\theta) \rangle, \quad (15)$$

$$h''_p(\theta) = |\gamma'(\theta)|^2 - \langle p - \gamma(\theta), \gamma''(\theta) \rangle. \quad (16)$$

A sufficient condition for θ_* to be a minimum of h_p is that $h'_p(\theta_*) = 0$ and $h''_p(\theta_*) > 0$ [17, Theorem 2.4]. Since the path

is regular, $h'_p(\theta_*) = 0$ is equivalent to $\varepsilon_\tau(p, \theta_*) = 0$, and by (10), to $(p, \theta_*) \in M$. Furthermore, for any \mathcal{C}^2 regular path,

$$\tau'(\theta) = |\gamma'(\theta)|\kappa(\theta)S\tau(\theta) = \frac{\gamma''(\theta)}{|\gamma'(\theta)|} - \frac{\langle \gamma''(\theta), \tau(\theta) \rangle \tau(\theta)}{|\gamma'(\theta)|}, \quad (17)$$

such that, for $(p, \theta) \in M$,

$$\langle p - \gamma(\theta), \gamma''(\theta) \rangle = |\gamma'(\theta)|^2 \kappa(\theta) \varepsilon_c(p, \theta). \quad (18)$$

It follows that if $(p, \theta_*) \in M$, then $h''_p(\theta_*) > 0$ is equivalent to $\kappa(\theta_*)\varepsilon_c(p, \theta_*) < 1$, and by (14), to $(p, \theta_*) \in O$. Consequently, the second order optimality conditions $h'_p(\theta_*) = 0$ and $h''_p(\theta_*) > 0$ are equivalent to $(p, \theta_*) \in O \cap M$. \square

For practical implementation purposes, a consequence of Proposition 1 is that we can choose the path parameter by solving an optimization problem at every discrete update step. In this way, we avoid the problem of θ drifting such that $(p, \theta) \notin M$. Moreover, for typical paths such as straight lines and circles, the minimizer of $\theta \mapsto |p - \gamma(\theta)|$ has a local closed-form solution as a function of p . However, solving an unconstrained optimization problem for the path parameter does not necessarily guarantee that the solution $t \mapsto \theta_*(t)$ is continuous. For instance, whenever the solution to the optimization problem becomes set-valued, a discontinuity can occur. When the path consists of straight line and circular segments, continuity of $t \mapsto \theta_*(t)$ can be ensured locally by introducing a memory variable, which accounts for which path segment one is currently on.

The second result pertaining to (13) concerns the existence of solutions. It turns out that solutions are guaranteed to exist locally if v is locally integrable. Furthermore, the completeness of maximal solutions can be guaranteed if the cross-track error remains sufficiently small relative to the path curvature.

Proposition 2. Let γ be a \mathcal{C}^2 regular path. If v is locally integrable, then there exists a solution to (13) from every initial condition in $O \cap M$. Moreover, every maximal solution to (13) whose range is confined to a set

$$C_r = \{(p, \theta) \in \mathbb{R}^3 : \kappa(\theta)\varepsilon_c(p, \theta) \leq r\}, \quad (19)$$

where $r < 1$, is complete.

Proof. Since γ is \mathcal{C}^2 regular, we can without loss of generality assume that γ is parametrized by arc length, such that $|\gamma'(\theta)| = 1$. Let $x := (p, \theta)$ and denote the flow map in (13) by $f : O \times \mathbb{R}^2 \rightarrow \mathbb{R}^3$. Since f is continuous and $t \mapsto v(t)$ is measurable, it holds that $t \mapsto f(x, v(t))$ is measurable for every $x \in O$. Furthermore, for every compact set $K \subset O$, there exists $k > 0$ such that $x \in K$ implies $|f(x, v)| \leq k|v|$. Since $t \mapsto k|v(t)|$ is locally integrable, the local existence of solutions follows from [18, Theorem 5.1]. Every solution $t \mapsto x(t)$ satisfies $\frac{d}{dt}\varepsilon_\tau(x(t)) = 0$ almost everywhere in its domain, such that solutions starting in M remain in M . If a maximal solution is confined to C_r for $r < 1$, then

$$|x(t)| \leq |x(0)| + \left(1 + \frac{1}{1-r}\right) \int_0^t |v(\eta)| d\eta \quad (20)$$

for every t in the solution's domain. Since v is locally integrable, finite escape does not occur, and such solutions must be complete. \square

IV. INTEGRAL LINE-OF-SIGHT GUIDANCE

Define a set-valued projection operator as in [19] by

$$\overline{\text{Proj}}(\sigma, \varphi, a) := \begin{cases} s\sigma & : \quad s = 1 \quad \text{if } \sigma \in \mathbb{T}_{[-a, a]}(\varphi) \\ & s \in [0, 1] \quad \text{if } \sigma \notin \mathbb{T}_{[-a, a]}(\varphi) \end{cases} \quad (21)$$

where the tangent cone $\mathbb{T}_{[-a, a]} : [-a, a] \rightrightarrows \mathbb{R}$ is defined by

$$\mathbb{T}_{[-a, a]}(\varphi) := \begin{cases} [0, \infty), & \text{if } \varphi = -a \\ (-\infty, \infty), & \text{if } \varphi \in (-a, a) \\ (-\infty, 0], & \text{if } \varphi = a \end{cases} \quad (22)$$

Consider the following projection-based ILOS guidance law

$$\dot{\alpha} \in \overline{\text{Proj}} \left(\frac{k\varepsilon_c(p, \theta)}{\sqrt{\Delta^2 + (\varepsilon_c(p, \theta) + \alpha)^2}}, \alpha, \bar{\alpha} \right), \quad (23a)$$

$$\mu(p, \theta, \alpha) = \frac{\Delta\tau(\theta) - (\varepsilon_c(p, \theta) + \alpha)S\tau(\theta)}{\sqrt{\Delta^2 + (\varepsilon_c(p, \theta) + \alpha)^2}}, \quad (23b)$$

where $\Delta > 0$ is the lookahead-distance, $k > 0$ represents an integral gain and $\bar{\alpha} \in \mathbb{R}$ denotes the maximum absolute value of the integral state. The control law (23b) can be rewritten as

$$\mu(p, \theta, \alpha) = R(\tau(\theta))\zeta(p, \theta, \alpha), \quad (24)$$

where ζ is the integral line-of-sight vector defined by

$$\zeta(p, \theta, \alpha) := \frac{1}{\sqrt{\Delta^2 + (\varepsilon_c(p, \theta) + \alpha)^2}} \begin{pmatrix} \Delta \\ -(\varepsilon_c(p, \theta) + \alpha) \end{pmatrix} \quad (25)$$

The angle representing μ on the interval $(-\pi, \pi]$ is equivalent to the sum of the angles corresponding to the unit vectors ζ and τ , mapped to the interval $(-\pi, \pi]$. However, operating with angles and their sums can be error-prone for implementation purposes. We advocate an implementation based on (23b) or (24), and then mapping the unit vector to an angle in $(-\pi, \pi]$ using the atan2 function if needed.

Remark 2. *With the angle interpretation of μ , the control law (23) is similar to AILOS as defined in [6] and the ILOS algorithm in [4]. The key difference is the introduction of the projection operator $\overline{\text{Proj}}$, which prevents integral wind-up by ensuring that the integral state α is bounded. Moreover, in an AILOS approach, the differential equation for the integral state α is proportional to the forward speed u_1 , which can be undesirable due to noisy velocity estimates.*

It might not be clear as to how one would implement the set-valued projection operator in (21). However, as discussed in [19], it turns out that we may use the discontinuous projection

$$\text{Proj}(\sigma, \varphi, a) := \begin{cases} \sigma, & \text{if } \sigma \in \mathbb{T}_{[-a, a]}(\varphi) \\ 0, & \text{if } \sigma \notin \mathbb{T}_{[-a, a]}(\varphi) \end{cases} \quad (26)$$

for implementation purposes. Additionally, if the differential equation (23a) is integrated using e.g. a forward Euler scheme,

employing Proj is equivalent to integrating the first argument in (23a) and saturating α at $\pm\bar{\alpha}$.

Applying the control law (23) to (1) and defining $x_1 := \varepsilon_c(p, \theta)$ results in the closed-loop cross-track error dynamics

$$\dot{x}_1 = \frac{-(x_1 + \alpha)u_1 + \Delta u_2}{\sqrt{\Delta^2 + (x_1 + \alpha)^2}} - |\gamma'(\theta)|\kappa(\theta)\varepsilon_\tau(p, \theta)\lambda(p, \theta, v). \quad (27)$$

Assume that γ is a C^2 regular path and that the path parameter can be selected such that it satisfies (13) with

$$v = u_1\mu(p, \theta, \alpha) + u_2S\mu(p, \theta, \alpha), \quad (28)$$

where μ is given by (23b). As a result, the along-track error ε_τ is zero at all times and the cross-track error dynamics are independent of θ . Thus, by defining $x_2 := \alpha - r$, where $r \in [-\bar{\alpha}, \bar{\alpha}]$ is the desired value of the integrator state α , we arrive at the error dynamics

$$\left. \begin{aligned} \dot{x}_1 &= \frac{-(x_1 + x_2)u_1 + \Delta u_2 - ru_1}{\sqrt{\Delta^2 + (x_1 + x_2 + r)^2}} \\ \dot{x}_2 &\in \overline{\text{Proj}} \left(\frac{kx_1}{\sqrt{\Delta^2 + (x_1 + x_2 + r)^2}}, x_2 + r, \bar{\alpha} \right) \end{aligned} \right\} \begin{array}{l} x \in X, \\ u \in U, \end{array} \quad (29)$$

where $X := \mathbb{R} \times [-\bar{\alpha} - r, \bar{\alpha} - r]$.

Theorem 1. *If $\rho > k$, then the origin is ISS for the system (29) with respect to the input $\xi_1(u) := |u_2 - \frac{r}{\Delta}u_1|$. Moreover, if u is such that $\xi_1(u) \leq \bar{\xi}_1$ for some $\bar{\xi}_1 \geq 0$, then the set*

$$\Omega_1 := \left\{ x \in X : (x_1 + x_2)^2 + x_2^2 \leq \left(\frac{\Delta\bar{\xi}_1}{\min(\rho - k, k)} \right)^2 \right\} \quad (30)$$

is forward invariant, and every solution $t \mapsto x(t)$ with initial condition $x_0 \in \Omega_1$ satisfies

$$|x_1(t)| \leq \frac{\sqrt{2}\Delta\bar{\xi}_1}{\min(\rho - k, k)}. \quad (31)$$

Proof. We consider the ISS Lyapunov function candidate $V_1(x) := \frac{1}{2}(x_1 + x_2)^2 + \frac{1}{2}x_2^2$. Then,

$$\dot{V}_1(x, u) = \frac{-(u_1 - ks)(x_1 + x_2)^2 - ksx_2^2 + (x_1 + x_2)(\Delta u_2 - ru_1)}{\sqrt{\Delta^2 + (x_1 + x_2 + r)^2}}. \quad (32)$$

If the integrator is not saturated, then $s = 1$, and

$$\dot{V}_1(x, u) = \frac{-(u_1 - k)(x_1 + x_2)^2 - ksx_2^2 + (x_1 + x_2)(\Delta u_2 - ru_1)}{\sqrt{\Delta^2 + (x_1 + x_2 + r)^2}}. \quad (33)$$

If the integrator is saturated, then $s \in [0, 1]$, and either $x_1 > 0$ and $x_2 = \bar{\alpha} - r \geq 0$, or $x_1 < 0$ and $x_2 = -\bar{\alpha} - r \leq 0$. In both cases, the product x_1x_2 is nonnegative, such that $(x_1 + x_2)^2 \geq x_2^2$. Consequently,

$$(u_1 - ks)(x_1 + x_2)^2 + ksx_2^2 \geq (u_1 - k)(x_1 + x_2)^2 + kx_2^2,$$

for all $s \in [0, 1]$, from which it follows that

$$\dot{V}_1(x, u) \leq \frac{-(u_1 - k)(x_1 + x_2)^2 - ksx_2^2 + (x_1 + x_2)(\Delta u_2 - ru_1)}{\sqrt{\Delta^2 + (x_1 + x_2 + r)^2}} \quad (34)$$

for all $(x, u) \in X \times U$. Letting $\chi \in (0, 1)$, it follows that

$$\dot{V}_1(x, u) \leq \frac{-2(1 - \chi)\min(\rho - k, k)V_1(z)}{\sqrt{\Delta^2 + 4V_1(z) + 2r^2}} \quad (35)$$

for all $x \in X$ such that $V_1(x) \geq \frac{1}{2} \left(\frac{\Delta \xi_1(u)}{\chi \min(\rho-k, k)} \right)^2$. This shows ISS of (29). Forward invariance of Ω_1 follows from noting that Ω_1 is a sublevel set of V_1 and that $\dot{V}_1(x, u) \leq 0$ for all $x \in X \setminus \Omega_1$. The bound (38) follows from inspection of Ω_1 . \square

Corollary 1. *If $u_1 \propto u_2$ and the conditions of Theorem 1 hold, then the origin is UGAS for (29).*

Proof. If $u_1 \propto u_2$, then $\frac{u_2}{u_1}$ is constant. Hence, we may choose $r = \Delta \frac{u_2}{u_1}$ and the claim follows from Theorem 1. \square

Assuming that u_1 and u_2 are proportional is equivalent to assuming that the crab angle $\beta = \text{atan2}(u_2, u_1)$ is constant, which is also assumed in the work on AILOS [6]. However, the work in [6] is based on the additional assumption that the crab angle is small, i.e., that $\frac{u_2}{u_1}$ is small.

The results in Theorem 1 and Corollary 1 also hold in the case where α is not saturated. A potentially sharper bound than (31), which exploits the saturation of the integrator, is given by the following proposition.

Proposition 3. *The compact set $\mathcal{A} = \{x \in X : x_1 = 0\}$ is ISS for (29) with respect to the input $\xi_2(u) := |\frac{u_2}{u_1}| + \frac{\bar{\alpha}}{\Delta}$. Moreover, if u is such that $\xi_2(u) \leq \bar{\xi}_2$ for some $\bar{\xi}_2 \geq 0$, then the set $\Omega_2 := \{x \in X : |x_1| \leq \Delta \bar{\xi}_2\}$ is forward invariant.*

Proof. We use $V_2(x) := \frac{1}{2} x_1^2$ as an ISS Lyapunov function candidate. Then, $\dot{V}_2(x, u) = \frac{-u_1 x_1^2 + x_1 (\Delta u_2 - (x_2 + r) u_1)}{\sqrt{\Delta^2 + (x_1 + x_2 + r)^2}}$. For $\chi \in (0, 1)$, we have that $\dot{V}_2(x, u) \leq \frac{-\rho(1-\chi)x_1^2}{\sqrt{\Delta^2 + 2x_1^2 + 2\bar{\alpha}^2}}$ for all $(x, u) \in X \times U$ satisfying $|x_1| \geq \Delta \xi(u)/\chi$, proving ISS. Forward invariance of Ω_2 follows from noting that Ω_2 is a sublevel set of V_2 and that $\dot{V}_2(x, u) \leq 0$ for all $x \in X \setminus \Omega_2$. \square

Remark 3. *Analogous results to Theorem 1, Corollary 1, and Proposition 3 can be derived for an AILOS version of (23), which utilizes, inspired by [6], the alternative integrator update law*

$$\dot{\alpha} \in \overline{\text{Proj}} \left(\frac{u_1 k_0 \varepsilon_c(p, \theta)}{\sqrt{\Delta^2 + (\varepsilon_c(p, \theta) + \alpha)^2}}, \alpha, \bar{\alpha} \right) \quad (36)$$

in place of (23a), where $k_0 \in (0, 1)$ is an integral gain. Specifically, the origin of the resulting error system is ISS with respect to the input $\xi_3(u) = |\frac{u_2}{u_1} - \frac{r}{\Delta}|$. If $\xi_3(u) \leq \bar{\xi}_3$, then the set

$$\Omega_3 := \left\{ x \in X : (x_1 + x_2)^2 + x_2^2 \leq \left(\frac{\Delta \bar{\xi}_3}{\min(1-k_0, k_0)} \right)^2 \right\} \quad (37)$$

is forward invariant. Furthermore, analogously to the bound (31) in Theorem 1, solutions $t \mapsto x(t)$ to the resulting closed-loop system starting in Ω_3 satisfy

$$|x_1(t)| \leq \frac{\sqrt{2} \Delta \bar{\xi}_3}{\min(1-k_0, k_0)}. \quad (38)$$

The conclusions of Corollary 1 and Proposition 3 hold without modification for the AILOS version of (23).

Theorem 1 and Proposition 3 yield bounds on the cross-track error, provided that we initialize the system close enough

to the path. These bounds can then be used to estimate an upper bound on the allowed curvature of the path to ensure that the path parameter can always be selected such that it satisfies (13). In other words, such that maximal solutions to (13) are complete as shown in Proposition 2. We can also think of the bounds in Theorem 1 and Proposition 3 as the maximum cross-track error incurred during operation of the vehicle under the given conditions.

V. CASE STUDY

The simulation model is a 6-degree-of-freedom model of the Remus 100 AUV from Kongsberg Maritime. In particular, the equations of motion of the vehicle are given by [20, Eqs. (8.1-8.2)] with model parameters taken from [21]. The control law (23) provides the desired heading for a lower-level heading autopilot, while the depth is kept constant by a proportional-integral controller which provides a pitch reference to a lower-level pitch autopilot. Finally, the roll motion is uncontrolled and passively stable.

We consider two cases; a straight-line path and a curved path in the form of a lemniscate. In both cases, we implemented (23) with and without the $\overline{\text{Proj}}$ operator, and we denote these versions as the saturated and unsaturated versions of (23), respectively. In both simulations, the propeller revolution is set to 550 revolutions per minute (rpm), which corresponds to a forward velocity of approximately 0.9 m/s in calm waters. The first simulation case is a simple straight-line example. The reference path is given by the x -axis and the vehicle is initialized at $p_0 = (-50 \text{ m}, 0)$. We include the effects of an ocean current with speed 0.2 m/s coming from the north. The parameters in (23) are chosen as $\Delta = 15 \text{ m}$, $k = 0.5$, $\bar{\alpha} = \tan(\beta_{\max})\Delta$, where $\beta_{\max} = 13 \frac{\pi}{180}$ represents the maximum crab angle when the cross-track error is zero.

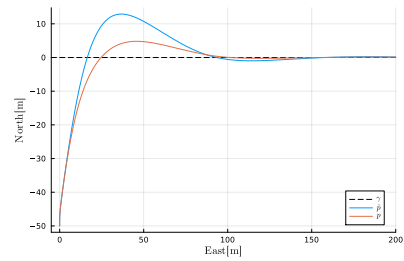


Fig. 1. The reference path γ and North-East trajectories p and \bar{p} obtained by setting the desired heading reference according to (23) with (red) and without (blue) the $\overline{\text{Proj}}$ operator, respectively.

From Fig. 1, we observe that for the saturated version, the initial overshoot is considerably smaller and the second overshoot is nonexistent. The second overshoot is a consequence of integral windup, as seen in the topmost left plot in Fig. 2, where the integral state becomes excessively large during the initial transient in the unsaturated approach. The lower left plot in Fig. 2 shows that by not saturating the integral state, the desired heading becomes smaller, and is hence more aggressive in the sense that it steers the vehicle straight towards the path, effectively lowering the lookahead distance.

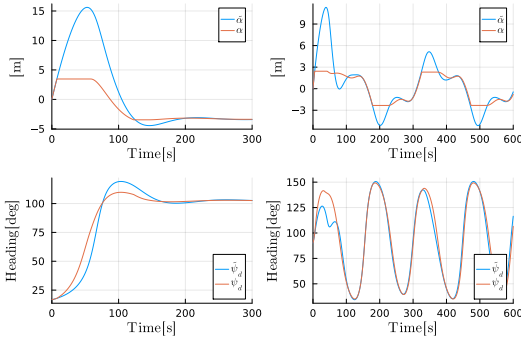


Fig. 2. The integral states α and $\tilde{\alpha}$ and the desired heading ψ and $\tilde{\psi}$ with (red) and without (blue) the use of the $\overline{\text{Proj}}$ operator, respectively. The leftmost plots correspond to the straight-line simulation case, while the rightmost plots correspond to the lemniscate simulation case.

The second simulation case is a lemniscate, which is a self-intersecting closed curved path. The vehicle is initialized at $p_0 = (0, 50 \text{ m})$, the ocean current speed is 0.3 m/s and is coming from the south. The parameters in (23) are chosen as in the previous case except $\Delta = 10 \text{ m}$ and $k = 0.7$.

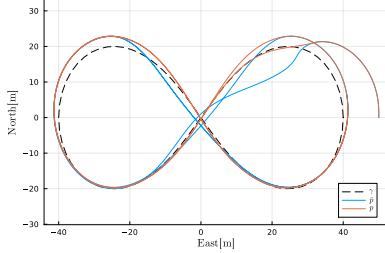


Fig. 3. The reference path γ and North-East trajectories p and \tilde{p} obtained by setting the desired heading reference according to (23) with (red) and without (blue) the $\overline{\text{Proj}}$ operator, respectively.

Similarly to the straight-line case, we observe in Fig. 3 that the transient behavior is significantly improved by employing the $\overline{\text{Proj}}$ operator in the control law. From Fig. 3 and the topmost right plot in Fig. 2, we see that the integral state of the unsaturated guidance law winds up during the sharp turns against the current, which results in overshoots on the straighter path segments near the origin. Despite the improved performance in the vicinity of the center of the lemniscate, both guidance laws still deviate significantly from the path when turning in following sea. This is due to the strong currents and large curvature of the path.

VI. CONCLUSIONS

This letter has presented a novel ILOS guidance scheme that results in a closed-loop system with ISS properties with respect to a function of the vehicle velocities. It has been shown that the origin of the closed-loop system is UGAS when the forward and sideways velocities are proportional. Importantly, and contrary to the state of the art, these global stability results have been established without requiring that the crab angle is small. Furthermore, we have discussed how to select the path parameter to ensure that the along-track error

remains zero for all time, and we have shown the connection between selecting the path parameter through an ODE and through optimization.

REFERENCES

- [1] N. Gu, D. Wang, Z. Peng, J. Wang, and Q.-L. Han, "Advances in line-of-sight guidance for path following of autonomous marine vehicles: An overview," *IEEE Transactions on Systems, Man, and Cybernetics: Systems*, vol. 53, no. 1, pp. 12–28, Jan. 2023.
- [2] E. Børhaug, A. Pavlov, and K. Y. Pettersen, "Integral LOS control for path following of underactuated marine surface vessels in the presence of constant ocean currents," in *Proc. 47th IEEE Conference on Decision and Control*. Cancun, Mexico: IEEE, 2008, pp. 4984–4991.
- [3] M. Bibuli, W. Caharija, K. Y. Pettersen, G. Bruzzone, M. Caccia, and E. Zereik, "ILOS guidance-experiments and tuning," *IFAC Proceedings Volumes*, vol. 47, no. 3, pp. 4209–4214, 2014.
- [4] W. Caharija, K. Y. Pettersen, M. Bibuli, P. Calado, E. Zereik, J. Braga, J. T. Gravdahl, A. J. Sorensen, M. Milovanovic, and G. Bruzzone, "Integral line-of-sight guidance and control of underactuated marine vehicles: Theory, simulations, and experiments," *IEEE Transactions on Control Systems Technology*, vol. 24, no. 5, pp. 1623–1642, Sep. 2016.
- [5] E. Kelasidi, P. Liljebäck, K. Y. Pettersen, and J. T. Gravdahl, "Integral line-of-sight guidance for path following control of underwater snake robots: Theory and experiments," *IEEE Transactions on Robotics*, vol. 33, no. 3, pp. 610–628, 2017.
- [6] T. I. Fossen, K. Y. Pettersen, and R. Galeazzi, "Line-of-sight path following for dubins paths with adaptive sideslip compensation of drift forces," *IEEE Transactions on Control Systems Technology*, vol. 23, no. 2, pp. 820–827, Mar. 2015.
- [7] A. M. Lekkas and T. I. Fossen, "Integral LOS path following for curved paths based on a monotone cubic hermite spline parametrization," *IEEE Transactions on Control Systems Technology*, vol. 22, no. 6, pp. 2287–2301, Nov. 2014.
- [8] L. Liu, D. Wang, and Z. Peng, "ESO-based line-of-sight guidance law for path following of underactuated marine surface vehicles with exact sideslip compensation," *IEEE Journal of Oceanic Engineering*, vol. 42, no. 2, pp. 477–487, Apr. 2017.
- [9] E. D. Sontag and Y. Wang, "On characterizations of the input-to-state stability property," *Systems & Control Letters*, vol. 24, no. 5, pp. 351–359, Apr. 1995.
- [10] T. I. Fossen, "An adaptive line-of-sight (ALOS) guidance law for path following of aircraft and marine craft," *IEEE Transactions on Control Systems Technology*, pp. 1–8, 2023.
- [11] T. I. Fossen and A. P. Aguiar, "A uniform semiglobal exponential stable adaptive line-of-sight (ALOS) guidance law for 3-D path following," *Automatica*, vol. 163, p. 111556, May 2024.
- [12] M. Marley, R. Skjetne, E. A. Basso, and A. R. Teel, "Maneuvering with safety guarantees using control barrier functions," *IFAC-PapersOnLine*, vol. 54, no. 16, pp. 370–377, 2021.
- [13] M. Marley, R. Skjetne, and A. R. Teel, "A kinematic hybrid feedback controller on the unit circle suitable for orientation control of ships," in *Proc. 59th Conf. on Decision and Control*, Jeju Island, Republic of Korea, 2020.
- [14] M. P. Do Carmo, *Differential Geometry of Curves and Surfaces*. Dover Publications, 2016.
- [15] P. Encarnacao and A. Pascoal, "3D path following for autonomous underwater vehicle," in *Proc. 39th IEEE Conference on Decision and Control*. Sydney, NSW, Australia: IEEE, 2000, pp. 2977–2982.
- [16] A. Micaelli and C. Samson, "Trajectory tracking for two-steering-wheels mobile robots," *IFAC Proceedings Volumes*, vol. 27, no. 14, pp. 249–256, Sep. 1994.
- [17] J. Nocedal and S. J. Wright, *Numerical Optimization*, 2nd ed. Springer, 2006.
- [18] J. K. Hale, *Ordinary Differential Equations*. Dover Publications, 2009.
- [19] E. A. Basso, H. M. Schmidt-Didlauskies, and K. Y. Pettersen, "Global asymptotic position and heading tracking for multirotors using tuning function-based adaptive hybrid feedback," *IEEE Control Systems Letters*, vol. 7, pp. 295–300, 2023.
- [20] T. I. Fossen, *Handbook of Marine Craft Hydrodynamics and Motion Control*, 2nd ed. Wiley, 2020.
- [21] T. I. Fossen and T. Perez, "Marine Systems Simulator (MSS)," 2004. [Online]. Available: <https://github.com/cybergalactic/MSS>